MARTIN MARIETTA

K/CSD/TM-78
Dist. Category UC-95

ANALYSIS OF SEVEN THERMAL BRIDGES IDENTIFIED IN A COMMERCIAL BUILDING

K. W. Childs

JUNE 1988

OPERATED BY
MARTIN MARIETTA ENERGY SYSTEMS, INC.
FOR THE UNITED STATES
DEPARTMENT OF ENERGY

Printed in the United States of America. Available from
National Technical Information Service
U.S. Department of Commerce
5285 Port Royal Road, Springfield, Virginia 22161
NTIS price codes—Printed Copy: A03 Microfiche A01

This report was prepared as an account of work sponsored by an agency of the United States Government. Neither the United States Government nor any agency thereof, nor any of their employees, makes any warranty, express or implied, or assumes any legal liability or responsibility for the accuracy, completeness, or usefulness of any information, apparatus, product, or process disclosed, or represents that its use would not infringe privately owned rights. Reference herein to any specific commercial product, process, or service by trade name, trademark, manufacturer, or otherwise, does not necessarily constitute or imply its endorsement, recommendation, or favoring by the United States Government or any agency thereof. The views and opinions of authors expressed herein do not necessarily state or reflect those of the United States Government or any agency thereof.

K/CSD/TM-78
Dist. Category UC-95

ANALYSIS OF SEVEN THERMAL BRIDGES IDENTIFIED IN A COMMERCIAL BUILDING

K. W. Childs

Computing and Telecommunications Division
at
Oak Ridge Gaseous Diffusion Plant
Post Office Box 2003
Oak Ridge, Tennessee 37831

Manuscript Completed - January 1988
Date Published - June 1988

Prepared for the
U.S. Department of Energy
Office of Buildings Energy Research and Development
Washington, DC 20555
No. EC010000

MARTIN MARIETTA ENERGY SYSTEMS, INC.
operating the
Oak Ridge National Laboratory
Oak Ridge Gaseous Diffusion Plant
Oak Ridge Y-12 Plant
Paducah Gaseous Diffusion Plant
for the
U.S. DEPARTMENT OF ENERGY
under contract DE-AC05-OR21400

CONTENTS

Page

LIST OF FIGURES iv

LIST OF TABLES v

ABSTRACT 1

INTRODUCTION 2

DEFINITIONS 2
IDENTIFICATION OF THERMAL BRIDGES 2

OCCURRENCE OF THERMAL BRIDGES 4

STEADY-STATE CALCULATIONS 8

BRIDGE 1 - PIPE SUPPORT 18
BRIDGE 2 - STEEL COLUMN 18
BRIDGE 3 - WINDOW WASHING PLATFORM SUPPORTING HOOK 20
BRIDGE 4 - FLOOR SLAB PERIMETER 20
BRIDGE 5 - STEEL STUD WALL 20
BRIDGE 6 - TWO-DIMENSIONAL FLOOR PENETRATION 21
BRIDGE 7 - THREE-DIMENSIONAL FLOOR PENETRATION 21

DYNAMIC CALCULATIONS 23

CORRECTIONS FOR THERMAL BRIDGES 27

SUMMARY AND CONCLUSIONS 29

ACKNOWLEDGMENTS 30

REFERENCES 31

LIST OF FIGURES

Figure		Page
1.	Examples of thermal bridges	5
2.	Heat flow in two-dimensional thermal bridge	6
3.	Bridge 1 - pipe support	9
4.	Bridge 2 - steel column	10
5.	Bridge 3 - window washing platform supporting hook	11
6.	Bridge 4 - floor slab perimeter	12
7.	Bridge 5 - steel stud wall	13
8.	Bridge 6 - two-dimensional floor penetration	14
9.	Bridge 7 - three-dimensional floor penetration	15

LIST OF TABLES

Table		Page
1.	Material conductivity	16
2.	Calculated steady-state thermal bridge results	17
3.	Calculated minimum interior surface temperature	19
4.	Average Y response factors	26
5.	Results of thermal bridge corrective measures	28

ABSTRACT

Seven thermal bridges occurring in a large modern office building are identified. The impact that these bridges have on building envelope heat flow and minimum interior surface temperature is investigated using a finite-difference heat transfer computer program. Assumptions that are made in the development of two- and three-dimensional numerical models are discussed. Steady-state numerical models are employed to determine parameters that can be used to calculate corrections to the values for heat flow and interior surface temperature obtained from one-dimensional analyses. The need for a means of characterizing the dynamic thermal response of bridges is also discussed, and two different numerical approaches to the calculation of response factors (or conduction transfer functions) are explored.

INTRODUCTION

DEFINITIONS

A Department of Energy workshop (ref. 1) on building envelope thermal anomalies (BETAs) produced the following definitions.

> A BETA is a material or configuration in a building that produces localized excessive heat flow from (or to) the building and a cold (or hot) area on an interior surface of the building.
>
> Excessive heat flow is heat flow beyond that normally modeled by traditional building energy analysis methods. Traditional methods assume spatial and temporal uniformity of elements and include one-dimensional conductance loss through wall segments, conductance through window glass, isothermal zone infiltration losses, forced ventilation losses, and radiation losses through glass areas. BETAs do not include phenomena caused by moisture accumulation.
>
> A thermal bridge is a BETA that is caused solely by heat conduction.

The definition of thermal bridges will be extended in this report to also include BETAs that contain narrow air gaps. Radiation can be an important heat transfer mechanism across gaps, and natural convection can become significant as the gap width increases. However, as long as the width of the gap is small, the heat transfer from one surface bounding the gap to the opposite surface can be represented by an effective conductance value that includes contributions due to conductivity, convection and radiation.

A building envelope component is a portion of a building envelope that is composed of one or more layers of material in which there is no variation in either composition or thickness.

IDENTIFICATION OF THERMAL BRIDGES

Thermal bridges have only become significant with the increase in typical insulation levels in building envelopes in recent years. In a majority of new construction there is a distinct, easily identified layer of insulating material in the building envelope. This layer embodies the predominant resistance to heat flow through the envelope. In general, a significant thermal bridge occurs where there is a discontinuity in this layer of insulation (i.e., there exists a heat flow path from the interior to the exterior of the envelope that does not entail heat conduction through insulation at all or entails heat conduction through a reduced thickness of insulation).

The steady-state heat flow in the vicinity of a thermal bridge obviously differs from that through the surrounding envelope, but the

dynamic behavior of a bridge can also be significantly different from the surrounding envelope. This different dynamic behavior between the bridge and the surrounding envelope can result in the interior surface heat flow near the bridge being out of phase with the heat flow through the remainder of the envelope. Both the steady-state and dynamic behavior can have an impact on the energy requirements for heating or cooling a building. In order to evaluate this impact the characteristics of the thermal bridge must be known.

If heating is required nearly continuously throughout a time period of interest, the dynamic behavior of a thermal bridge need not be known in order to obtain a realistic estimate of total heating energy requirements over that period. For this situation knowledge of the steady-state characteristics is sufficient to allow determination of total heating requirements. Hourly heating requirement estimates cannot be made accurately with only this information. If heating is not required nearly continuously in a building containing significant thermal bridges, then it is necessary to characterize the dynamic thermal behavior of the bridges.

Excessive heat flow is not the only, or necessarily the most important, consequence of a thermal bridge in a building. In cold weather a thermal bridge can produce a localized region of low temperature on the inside surface of a building envelope. This low-temperature area can result in condensation of moisture from the interior air which, in turn, can lead to mold growth, staining, and possible deterioration of interior finishing materials.

Building designers can recognize a design detail that constitutes a thermal bridge, but they often do not have the means to assess the impact or compare performance relative to an alternative design detail. As a first step toward developing a simple method for assessing thermal bridges, a detailed study of thermal bridges in a large modern office building was undertaken. As part of this study seven thermal bridges were identified from the building drawings and verified by on-site inspection using infrared thermography. The overall project is documented in ref. 2, but this report gives a more detailed account of the analyses of the thermal bridges in isolation from the remainder of the building.

OCCURRENCE OF THERMAL BRIDGES

Two-dimensional thermal bridges occur where a building envelope component is intersected by another building component (either another envelope component, an internal building component such as a floor or partition, or a structural component). The nature of any bridge occurring at this intersection is revealed by examining a cross section of the envelope perpendicular to the line of intersection. This cross section does not vary along the line of intersection. Examples of this type of thermal bridge are illustrated in Fig. 1. Part (a) illustrates an interior building component penetrating the envelope insulating layer, and part (b) illustrates a corner formed by the juncture of two envelope components. Even if the insulation were not completely absent but only reduced in thickness, these could still be significant thermal bridges.

Consider the example shown in Fig. 2 where the envelope is penetrated by a thermal bridge. There is two-dimensional heat flow near the bridge, but the two-dimensional effects diminish with distance from the bridge until, at some point, the heat flow can be considered one-dimensional. Any plane sectioning the envelope perpendicular to its surfaces in a region where the heat flow is one-dimensional is adiabatic. Adiabatic planes may also result from symmetry when a building detail is repeated. Two adiabatic planes (one on either side of the bridge) delineate a portion of the envelope containing the thermal bridge that can be analyzed independent of the remainder of the envelope. Finite element or finite difference numerical analysis techniques can be used to determine the steady-state heat flow rate through the portion of the envelope containing the thermal bridge.

A thermal bridge, as illustrated in Fig. 1 (a), occurs where a floor in a multistory building or an interior partition penetrates the envelope insulation. In order to analyze this thermal bridge it must be delineated from the rest of the building by three adiabatic planes. The additional plane cuts the floor or partition at a point far enough removed from the envelope that the heat flow is negligible.

Thermal bridges with three-dimensional heat flow occur where a corner formed by two envelope components is intersected by a floor or roof. They also occur where the intersection of a structural component and the envelope occurs in a localized region rather than along a line (e.g., a beam perpendicular to the envelope component it penetrates). An envelope component penetrated by a structural component with a circular cross section does not result in a three-dimensional bridge (heat flow is two-dimensional when viewed in an r-z cylindrical coordinate system.) For the purpose of analysis, the region containing the thermal bridge can be isolated from the remainder of the building by the identification of a set of adiabatic surfaces. The isolated portion of the envelope containing the bridge can then be analyzed using a finite element or finite difference computer program to determine the total heat flow rate.

DWG. NO. K/G-88-02
(U)

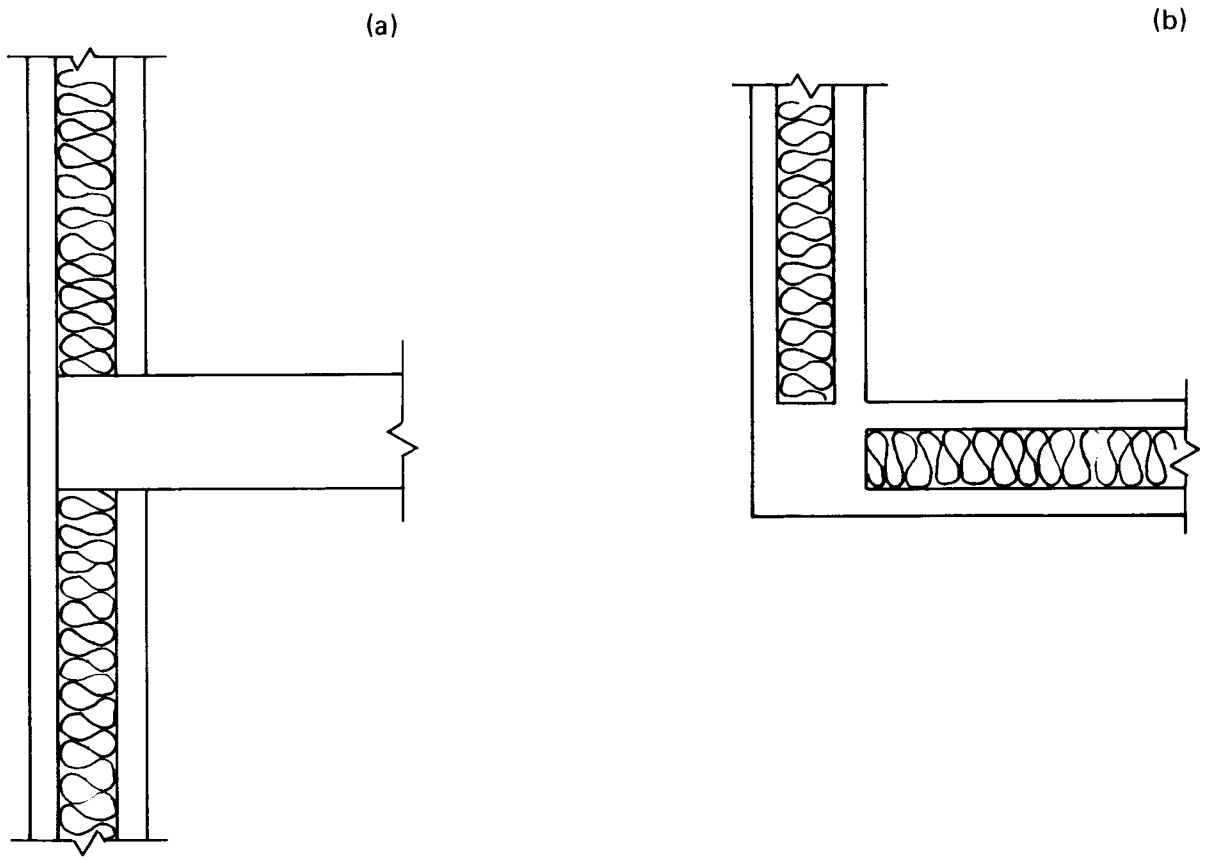

Fig. 1. Examples of thermal bridges.

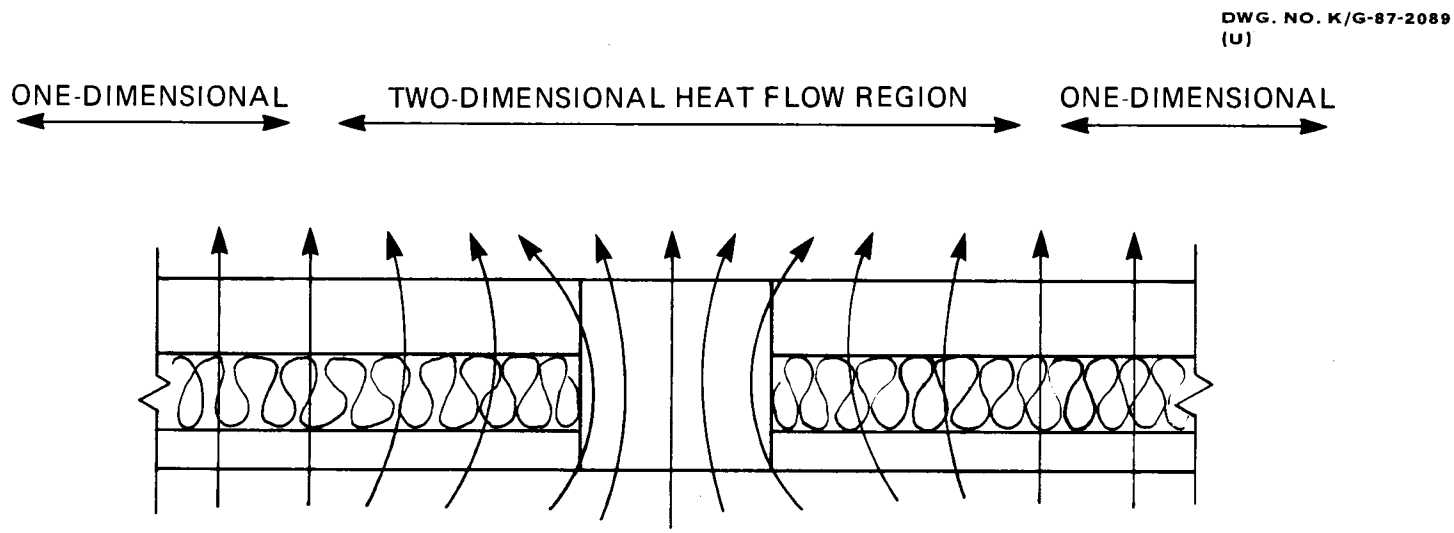

Fig. 2. Heat flow in two-dimensional thermal bridge.

Actual thermal bridges are often much more complex than the simple thermal bridges used to illustrate the concepts discussed in this section. The identification of truly adiabatic planes is not always possible, and geometric simplification of a bridge is often necessary in order to make the thermal analysis practical. The validity of the calculated results is dependent on the expertise of the heat transfer analyst who does the modeling.

STEADY-STATE CALCULATIONS

This section presents the analyses of seven thermal bridges identified in a multistory office building (ref. 2). These bridges are illustrated in Figs. 3 through 9. All of the analyses were performed with the finite difference heat transfer code HEATING6 (ref. 3). Convective heat transfer coefficients of 1.47 and 5.88 Btu/h•ft^2•°F were used on the inside and outside surfaces, respectively. The conductivity of all materials was assumed to be constant with the values given in Table 1. Surface-to-surface heat transfer across air gaps is modeled using a constant conductance value of 0.67 Btu/h•ft^2•°F. Contact resistances at the interfaces between materials are neglected. Additional modeling assumptions that are specific to each bridge are discussed below.

The results of the calculations for all seven bridges are presented in Table 2. The first column in the table gives the bridge identification number. The second column lists the envelope interior surface area that is included in the numerical model. For several of the bridges, symmetry conditions allow the numerical model to encompass only one-half or one-quarter of the thermal bridge. The values listed are the interior surface areas that would have been included in the model if symmetry conditions had not been used. The third column is the calculated heat flow through the bridge and the surrounding portion of the envelope for a 1°F interior/exterior air temperature difference. This value was obtained by integrating the surface heat flux over all surfaces exposed to the exterior (or interior) boundary condition and dividing by the temperature difference applied. The heat flow was calculated for both the interior and exterior and compared to confirm that steady-state conditions had indeed been achieved. The fourth column gives the R-value of the building envelope if the bridge were not present. The fifth column is an effective R-value for the bridge and surrounding portion of the envelope. This value is obtained by dividing column 2 by column 3. The sixth column is an excess conductance due to the thermal bridge that can be used as a correction to the heat flow obtained from a one-dimensional calculation. For a two-dimensional thermal bridge the product of the excess bridge conductance, the length of the bridge, and the indoor/outdoor temperature difference gives the discrepancy between that actual heat flow and the heat flow through the envelope in the absence of the bridge. For a three-dimensional bridge, the product of the bridge conductance and the indoor/outdoor temperature difference gives the heat flow correction.

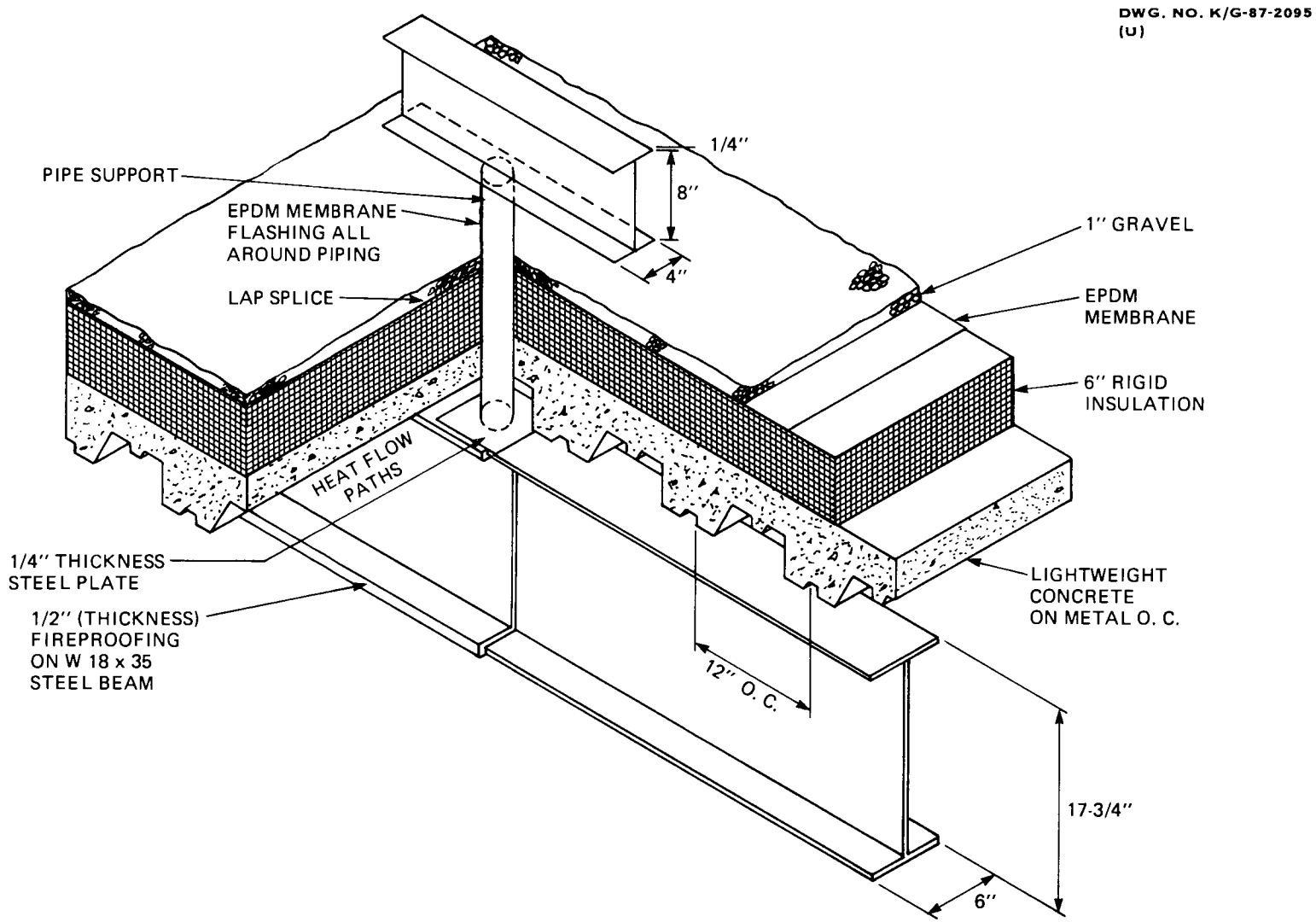

Fig. 3. Bridge 1 - pipe support

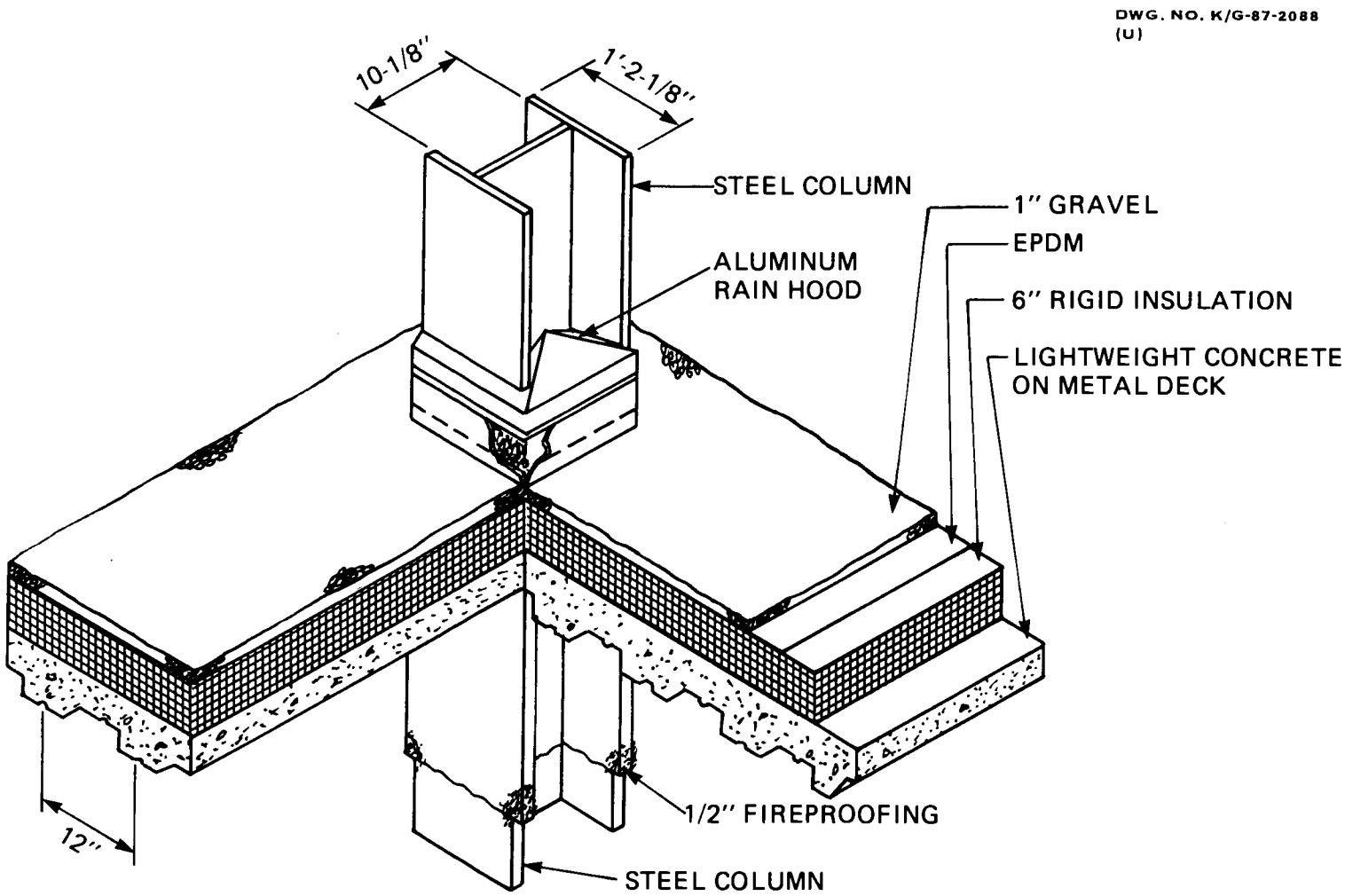

Fig. 4. Bridge 2 - steel column.

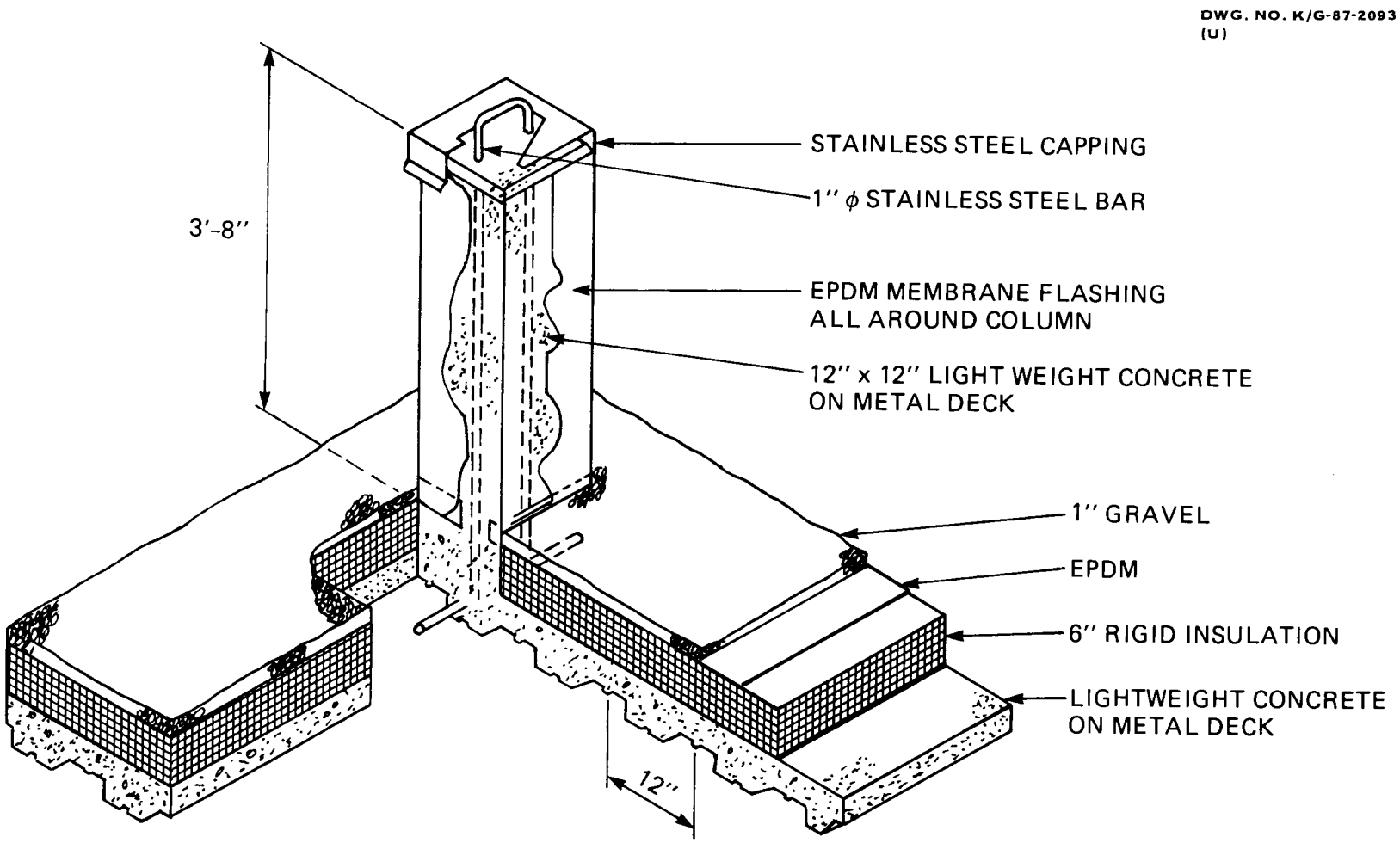

Fig. 5. Bridge 3 - window washing platform supporting hook.

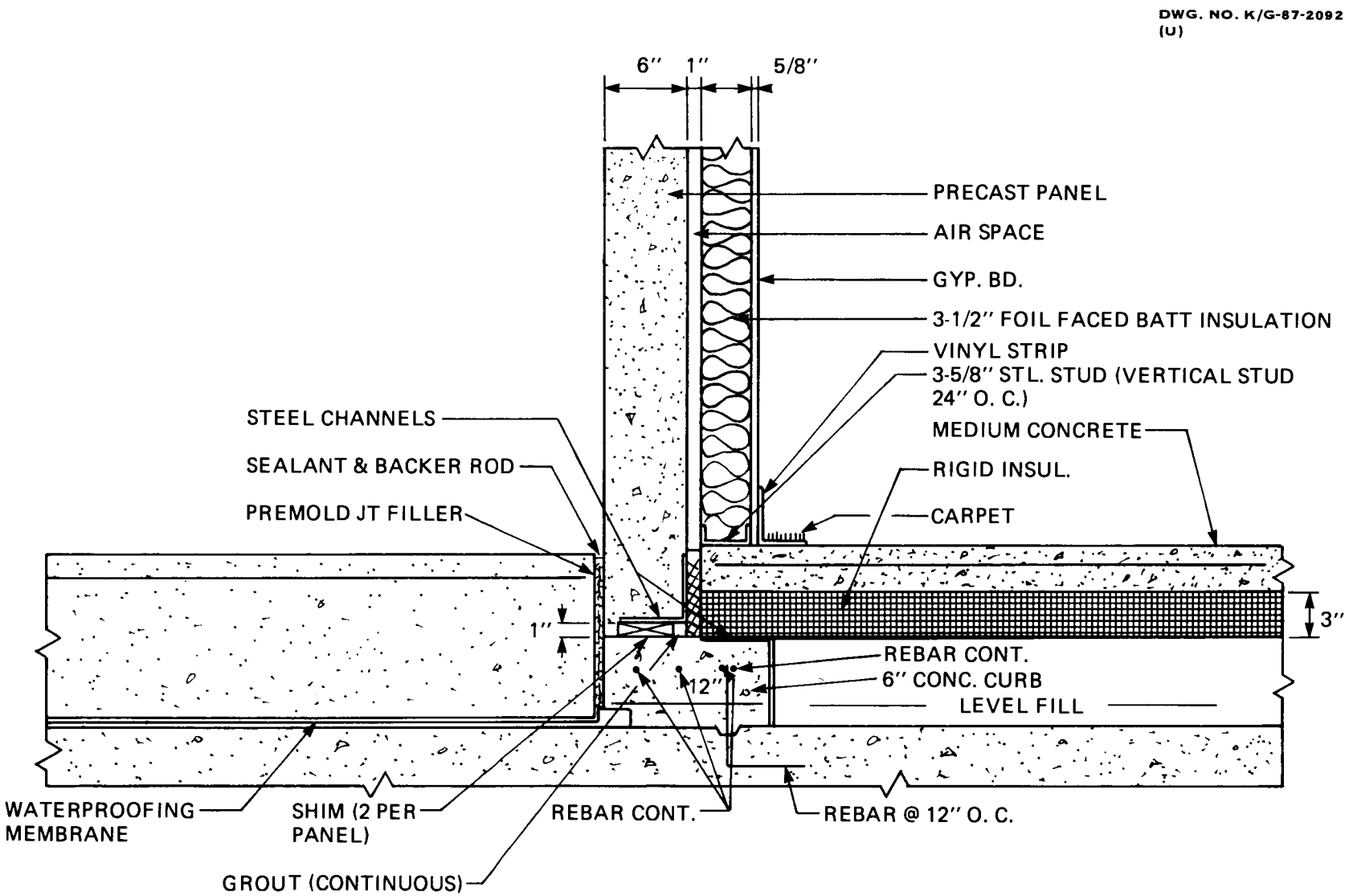

Fig. 6. Bridge 4 - floor slab perimeter.

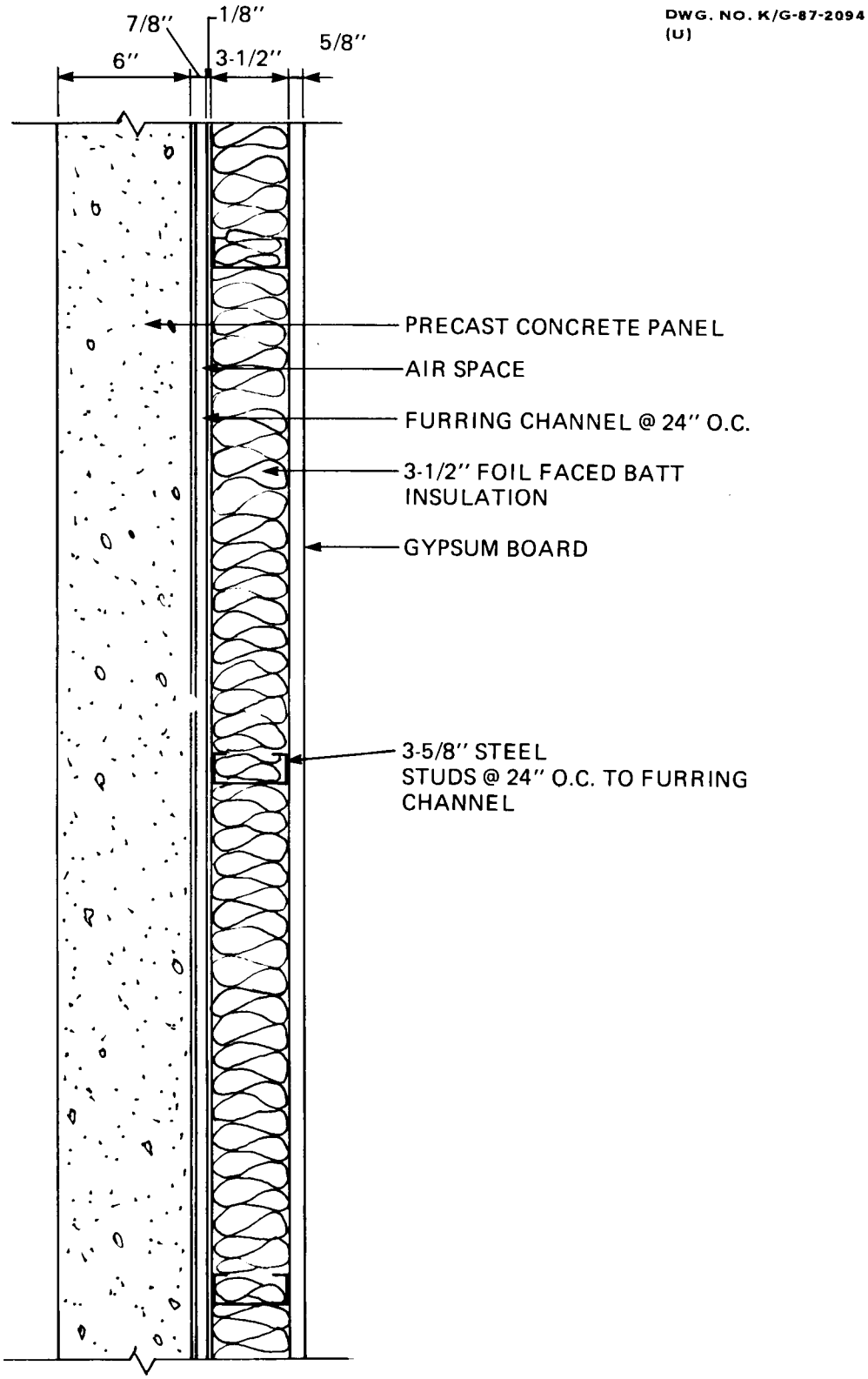

Fig. 7. Bridge 5 - steel stud wall.

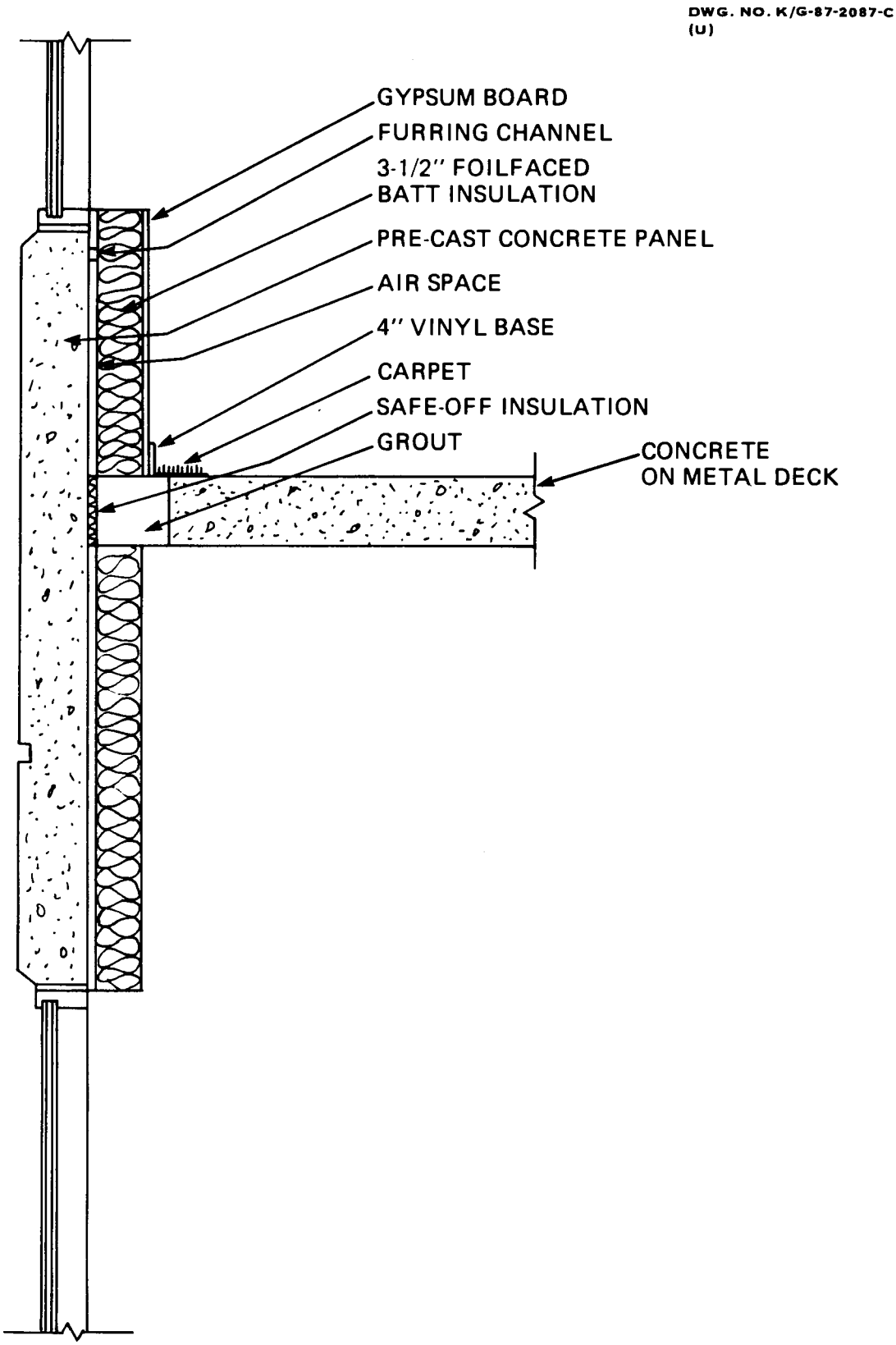

Fig. 8. Bridge 6 - two-dimensional floor penetration.

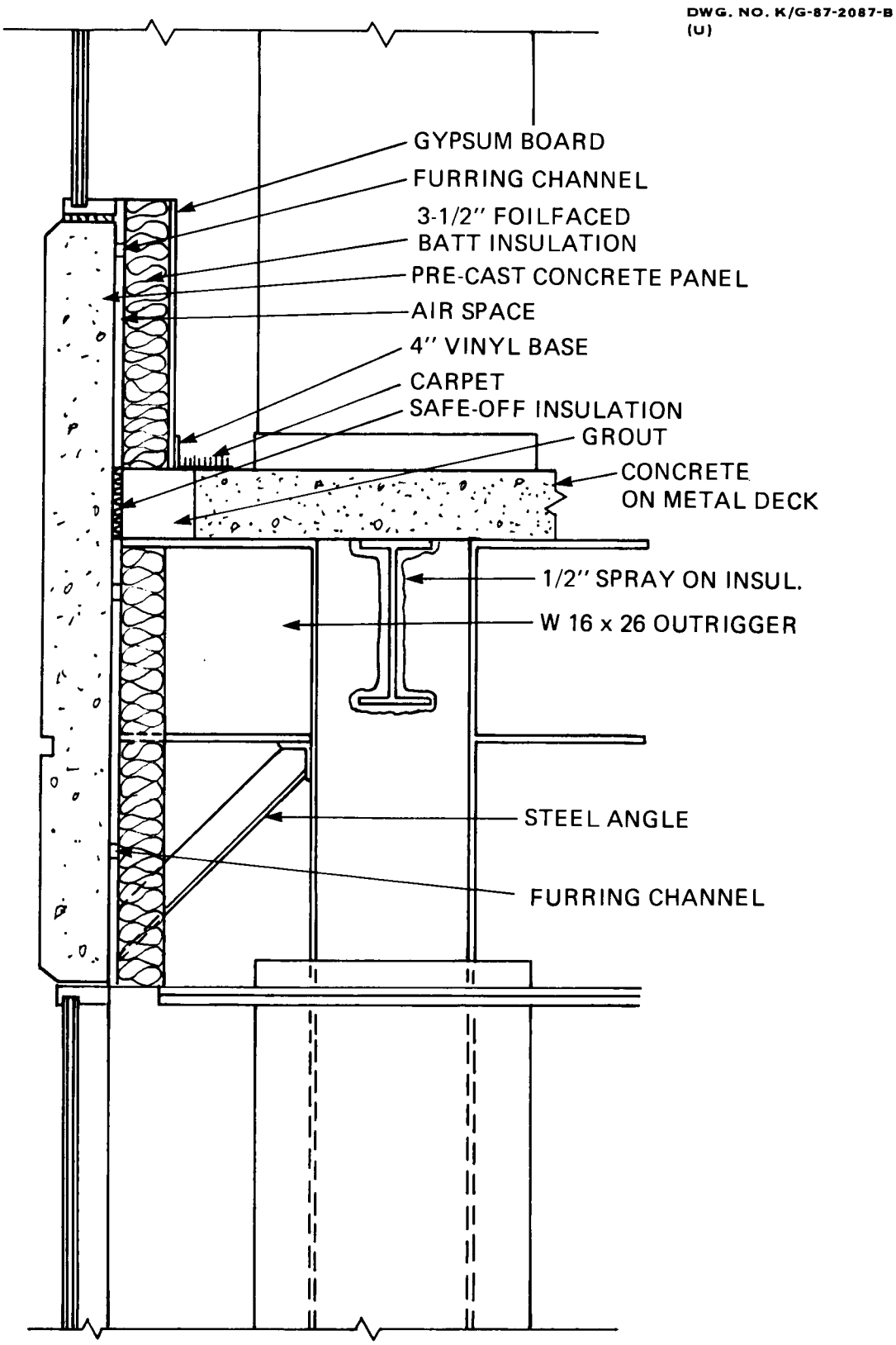

Fig. 9. Bridge 7 - three-dimensional floor penetration.

Table 1. Material conductivity

Material	Conductivity (Btu/h•ft•°F)
Concrete (roof)	0.542
Concrete (floor)	1.255
Grout	1.255
Stone ballast (roof)	0.834
Steel	25.0
Stainless steel	11.0
Gypsum board	0.0926
EPDM roofing membrane	0.1
Pourable sealer	1.2
Rigid insulation	0.021
Batt insulation	0.025
Fireproofing	0.13
Dry compacted earth	0.037
Carpet/pad	0.1

Table 2. Calculated steady-state thermal bridge results

1	2		3	4	5	6	
Bridge No.	Envelope interior surface area in model		Calculated heat flow	Undisturbed R-value	Effective R-value	Excess bridge conductance	
	ft^2	$\frac{ft^2}{ft \text{ of length}}$	$\frac{Btu}{h \cdot °F}$	$\frac{h \cdot ft^2 \cdot °F}{Btu}$	$\frac{h \cdot ft^2 \cdot °F}{Btu}$	$\frac{Btu}{h \cdot °F}$	$\frac{Btu/h \cdot °F}{ft \text{ of length}}$
1	16	--	1.11	25.5	14.4	0.48	--
2	16	--	3.63	25.5	4.4	3.01	--
3	16	--	1.19	25.5	13.4	0.57	--
4	--	2	0.33	14.9	6.1	--	0.19
5	4	--	0.40	14.9	10.1	0.13	--
6	--	3	0.46	14.6[a]	6.5[b]	--	0.26
7	24	--	4.02	14.5[a]	6.0[c]	0.78[d]	--

[a]Area weighted average of different envelope R-values above and below floor slab (14.9 above, 14.3 below).

[b]R = 7.6 based on envelope exterior surface area.

[c]R = 6.7 based on envelope exterior surface area.

[d]Excess conductance for bridge is 2.34. Value shown has conductance for 6 ft of two-dimensional bridge 6 subtracted (2.34 - 6 x 0.26 = 0.78).

A by-product of a finite-element or finite-difference heat transfer analysis is the temperature distribution in the vicinity of the thermal bridge from which the minimum surface temperature can be determined. The minimum interior surface temperature can be represented as the dimensionless quantity

$$\theta = \frac{T_m - T_o}{T_i - T_o} ,$$

where

T_i = indoor air temperature,
T_o = outdoor air temperature,
T_m = minimum inside surface temperature.

If θ is known, this equation can be solved for the minimum interior temperature occurring for any combination of indoor and outdoor temperatures. This can be used to determine how often the interior surface temperature falls below the indoor dew point during the winter, and consequently how severe the impact will be. The dimensionless minimum interior surface temperature for each bridge is given in Table 3. The dimensionless interior temperature for the envelope component without the bridge is also given for comparison.

BRIDGE 1 - PIPE SUPPORT

Bridge 1 (Fig. 3) is a pipe penetrating the roof insulation. The pipe is used to support mechanical equipment located on the roof of the building. This bridge requires a three-dimensional heat transfer analysis. The portion to be modeled is delineated from the remainder of the building by the identification of four adiabatic planes that form the sides of a square box, with the pipe penetration in the center. The square is 4 ft along each side. The portions of the I-beams within this box were included in the model. Due to planes of symmetry only one-quarter of the bridge was included in the numerical model. Several simplifications are made in the numerical model as compared to the actual bridge: the round pipe is modeled as a square pipe having the same cross-sectional area, the EPDM membrane is not included, and the complicated contour of the steel deck is modeled as a square wave. The resulting finite-difference model contained 1100 nodes.

BRIDGE 2 - STEEL COLUMN

Bridge 2 (Fig. 4) is a steel I-beam penetrating the roof insulation. The I-beam is used to support mechanical equipment located on the roof of the building. Six adiabatic planes are required to delineate a portion of the roof containing the thermal bridge to be modeled. Four of the planes are similar to the planes identified for the previous bridge. The other two planes are horizontal planes that cut the I-beam 2 ft above the top of the roof and 2 ft below the deck. As in the previous bridge the presence of symmetry allows the numerical model to encompass only one-quarter of the

Table 3. Calculated minimum interior surface temperature

Bridge No.	Minimum dimensionless interior surface temperature	
	Undisturbed	With bridge
1	0.97	0.80
2	0.97	0.73
3	0.97	0.82
4	0.96	0.57
5	0.96	0.78
6	0.96	0.74
7	0.96	0.72

bridge. Simplifications used in the numerical modeling of this bridge are the following: the aluminum rain hood is not included, the EPDM membrane is not modeled, and the concrete is modeled as having a uniform thickness equal to the average thickness of the actual case. The resulting finite-difference model contains 496 nodes.

BRIDGE 3 - WINDOW WASHING PLATFORM SUPPORTING HOOK

Thermal bridge 3 (Fig. 5) is a window washing platform support hook consisting of a concrete pillar penetrating the roof insulation. Contained within the concrete pillar is a stainless steel bar. Four adiabatic planes are required to delineate this bridge from the surrounding roof. These planes form a square, 4 ft on a side, with the pillar at the center. Symmetry conditions allow the numerical model to encompass only one-quarter of the actual bridge. The following simplifications are used in the numerical modeling of this bridge: the stainless steel capping is not modeled, the EPDM membrane is not modeled (the EPDM membrane used as flashing around the column is included in the model by modifying the surface heat transfer coefficient), the concrete is modeled as having a uniform thickness, and the round stainless steel bar is modeled as a square bar with the same cross-sectional area. The resulting finite-difference model contains 1451 nodes.

BRIDGE 4 - FLOOR SLAB PERIMETER

Thermal bridge 4 is the intersection of the ground floor slab with the exterior wall of the building. Four adiabatic planes are required to delineate the portion containing the thermal bridge from the remainder of the building. The portion of the building included in the numerical model of the bridge is depicted by Fig. 6. Three of the planes delineating the portion to be modeled (the two vertical planes cutting the floor and the horizontal plane cutting the wall) can be considered adiabatic if they are far enough removed from the bridge, but the forth plane (defining the lower extent of the model) is not truly an adiabatic plane. There may be heat flow to or from the ground below the structure crossing this plane. However, for the purpose of calculating heat flow from the interior air to the exterior air, this plane is modeled as adiabatic. These additional simplifying assumptions are made in developing the numerical model: steel shims supporting the precast panel are not modeled, reinforcing bars in the concrete are not modeled, waterproofing membrane is not modeled, and the vertical steel studs in the interior insulating wall are not modeled. The finite-difference model contains 298 nodes.

BRIDGE 5 - STEEL STUD WALL

Bridge 5 is an insulated, steel stud wall on the interior of a precast concrete panel. Figure 7 shows a horizontal cross-section of the wall. Horizontal, steel furring strips spaced 24 in. apart are attached to the precast concrete panel. Vertical, steel studs spaced 24 in. apart are in turn attached to the furring strips. The locations where the steel studs are attached to the furring channels are on a square grid, repeating every

two feet both horizontally and vertically over the entire surface of the envelope. Examining a 2 ft^2 portion of the envelope centered at the stud/channel connection reveals a pattern that occurs repeatedly over the entire envelope. Due to symmetry the four planes forming this square are adiabatic. Two of the planes are vertical planes that lie midway between a stud and the adjacent studs on either side. The other two are horizontal planes that lie midway between a furring channel and the adjacent channels above and below. This square delineates a single three-dimensional bridge that is repeated for every 4 ft^2 of envelope surface area. Due to additional symmetry only one-half of the bridge need be included in the numerical model. If the studs had been attached directly to the precast concrete panel rather than to furring strips, two-dimensional bridges would have resulted. The finite-difference model contains 2413 nodes.

BRIDGE 6 - TWO-DIMENSIONAL FLOOR PENETRATION

Bridge 6 is shown in Fig. 8. The thermal bridge of primary interest is the concrete floor and steel deck penetrating the insulation layer. Additional thermal bridges occur at the window frames and where steel studs are used in the interior insulating wall. Three adiabatic planes are necessary to delineate the bridge of primary interest from the rest of the building for analysis. A vertical plane cutting the floor slab at some location far removed from the exterior wall is one of these planes. Due to the close proximity of the window frames to the floor penetration, there may not be any horizontal adiabatic planes between the floor penetration and the windows. The numerical model could be extended to include a portion of the windows where adiabatic planes do exist, but instead arbitrary planes were chosen that were considered to be nearly adiabatic. This choice was made for two reasons: details in the vicinity of the window frame were not readily available, and, even if they were, including the additional bridges in the numerical model would make it difficult to distinguish the impact of the bridge of primary interest. The two portions of the envelope included in the numerical model extended 1.5 ft above the top and 1.5 ft below the bottom of the floor slab. The following simplifying assumptions were made in developing the numerical model: the steel furring strips and studs in the interior insulating wall were not included nor was the slot in the precast concrete panel. The finite-difference model contains 368 nodes.

BRIDGE 7 - THREE-DIMENSIONAL FLOOR PENETRATION

Bridge 7 (Fig. 9) is similar to bridge 6, but it is at a location where an outrigger boom (steel I-beam) supports the precast concrete panel. These booms are spaced every 30 ft around the perimeter of the building. Simplifying assumptions similar to those discussed for bridge 6 were also made for this bridge. Two additional adiabatic planes are required to delineate this bridge from the remainder of the building. These planes were assumed to be 3 ft from the vertical centerline of the I-beam on either side. Due to symmetry only one-half of the bridge needed to be

included in the numerical model. The finite-difference model for this bridge contains 6268 nodes. This is a composite thermal bridge consisting of a three-dimensional bridge superimposed on a two-dimensional bridge. The excess bridge conductance listed in Table 2 is only that attributable to three-dimensional conduction. The excess conductance due to the 6 ft of two-dimensional bridge 6 contained in bridge 7 has been subtracted.

DYNAMIC CALCULATIONS

For one-dimensional problems an exact solution is possible for linear heat transfer through multilayer envelope components. The only necessary simplifications are that all properties are assumed to be constant and the time variation in boundary temperatures is approximated by a series of straight line segments (resulting from the sum of a series of overlapping triangular pulses). The boundary temperatures used in the solution may be either the temperatures on the inner and outer surfaces of the envelope component or the indoor and outdoor air temperatures. However, the air temperatures can be used only if the heat flux at the surface is a linear function of the air/surface temperature difference. The solution can be expressed as a pair of algebraic expressions which give the heat flux on either surface of the envelope as a linear function of current and past boundary temperatures. The coefficients in this expression are obtained from the exact solution and are referred to as response factors. For nonlinear boundary conditions such as radiation, surface-to-surface response factors can be used and the resulting linear algebraic equation can be solved simultaneously with the nonlinear boundary condition equation.

A variation on the response factor uses the past heat fluxes as well as the current and past boundary temperatures. The coefficients for this method are referred to as conduction transfer functions. Less past history is required for the same degree of accuracy when conduction transfer functions are used in place of response factors.

Thermal bridges entail two- or three-dimensional heat flow, and an exact solution is not feasible for any but the simplest case. Ceylan and Myers (ref. 4) and Seem et al. (ref. 5) have, however, developed approximate methods for obtaining two- or three-dimensional conduction transfer functions. In both approaches the domain of the thermal bridge is discretized using either a finite-difference or finite-element approach. This discretization introduces an approximation that was not required for one-dimensional problems. An exact solution to the resulting system of first-order ordinary differential equations is then obtained. The method of solution used by Seem differs from that of Ceylan and Meyers, but they are conceptually very similar. Air-to-air transfer functions can be determined for a portion of an envelope containing a two- or three-dimensional thermal bridge using one of these methods. These transfer functions can be used by a building energy use computer program since they are identical in nature to transfer functions for one-dimensional envelope components.

In the following discussion the term response factor will be used in a broader sense to include conduction transfer functions. Air-to-air response factors do not allow any time or temperature dependence in the surface film coefficients. This situation precludes the direct modeling of radiation or time varying wind conditions. This shortcoming can be overcome in one-dimensional problems by use of surface-to-surface response factors, as already mentioned. However, a significant spatial variation in surface temperature is a common characteristic of thermal bridges. Thus, unlike a one-dimensional envelope component, there is not a single surface temperature, but a surface temperature distribution that must be

considered. The surface temperature distribution depends on both the bridge characteristics and on the boundary condition applied to it. Thus, it may not be possible to arrive at values for surface-to-surface response factors for thermal bridges that are independent of the boundary conditions applied. However, it may be possible to arrive at approximate surface-to-surface response factors that are applicable over a range of boundary conditions.

The method of Ceylan and Myers, as well as that of Seem et al., involves the manipulation of n x n matrices, where n is the number of nodes in the numerical model. Thus, the computer storage requirements go up as the square of the number of nodes. Even on many mainframe computers, available storage will limit the largest problem that can be solved to a few hundred nodes. This number of nodes is adequate for simple to moderately complex two-dimensional thermal bridges, but is probably insufficient for any but the simplest three-dimensional thermal bridge.

An alternative approach that requires considerably less computer storage, but more computing time, is used to calculate response factors for this report. This approach makes use of the transient analysis capability available in many existing finite-difference or finite-element heat transfer computer programs. A transient calculation is performed on a bridge of interest with a triangular pulse in the outdoor air temperature and the indoor air temperature held fixed. Air film resistances used in the calculations are 0.17 $h \cdot ft^2 \cdot °F/Btu$ on the outside and 0.68 $h \cdot ft^2 \cdot °F/Btu$ on the inside. The Y response factors are obtained for hourly time steps by integrating the heat flux over the inner surface at each hour in the transient and dividing by the projected interior surface area. The hourly integrated heat fluxes are obtained from a transient calculation with HEATING6 using a Crank-Nicolson implicit solution technique. The time step used in the HEATING6 calculation is initially much smaller than the 1-h time step in the calculated response factors and is increased as the transient progresses. This approach is attractive for obtaining results fairly quickly since there is no new software development required. The Y response factors obtained are an average value for the modeled area in the vicinity of the bridge; they do not represent the actual heat flow at any specific location. These average Y response factors for thermal bridges 2, 3, and 4 are presented in Table 4.

The duration of the transient calculation that must be performed can probably be reduced significantly — with a corresponding reduction in computer costs — by using a different outdoor air temperature input history and not obtaining the response factors directly. The calculated heat flow histories could be used to determine response factors in a subsequent step. This procedure is analogous to running an experiment in a hot box and calculating the response factors from the measured heat flow histories. A computer program capable of performing this necessary calculation is not currently available, but researchers at the National Bureau of Standards and at the National Research Council of Canada, among others, are exploring this area.

Response factors or conduction transfer functions are not of much direct interest to a building designer. However, they can be used by an analyst to model the dynamic impact of thermal bridges on whole building energy performance using one of the available whole building energy use computer models. The information from these analyses would be of use to building designers in making decisions about thermal bridges.

Table 4. Average Y Response Factors

	Bridge 2	Bridge 3	Bridge 4
Effective area, ft^2	16	16	2 × Perimeter
$U_{average}$, $Btu/h \cdot ft^2 \cdot °F$	0.2267	0.0749	0.2171
$R_{average}$, $h \cdot ft^2 \cdot °F/Btu$	4.41	13.35	4.61

i	Bridge 2	Bridge 3	Bridge 4
0	1.148462×10^{-3}	1.366609×10^{-4}	2.297773×10^{-4}
1	1.265007×10^{-2}	1.709966×10^{-3}	3.909038×10^{-3}
2	2.445254×10^{-2}	3.730974×10^{-3}	1.012997×10^{-2}
3	2.777850×10^{-2}	4.823214×10^{-3}	1.308086×10^{-2}
4	2.621965×10^{-2}	5.210118×10^{-3}	1.304388×10^{-2}
5	2.290978×10^{-2}	5.230837×10^{-3}	1.192066×10^{-2}
6	1.930492×10^{-2}	5.061552×10^{-3}	1.060840×10^{-2}
7	1.598669×10^{-2}	4.791484×10^{-3}	9.384412×10^{-3}
8	1.313890×10^{-2}	4.469767×10^{-3}	8.308493×10^{-3}
9	1.077563×10^{-2}	4.125779×10^{-3}	7.378429×10^{-3}
10	8.846176×10^{-3}	3.777968×10^{-3}	6.577463×10^{-3}
11	7.281948×10^{-3}	3.438068×10^{-3}	5.887330×10^{-3}
12	6.015984×10^{-3}	3.113403×10^{-3}	5.291491×10^{-3}
13	4.989995×10^{-3}	2.808292×10^{-3}	4.775703×10^{-3}
14	4.155861×10^{-3}	2.524990×10^{-3}	4.327894×10^{-3}
15	3.474907×10^{-3}	2.264338×10^{-3}	3.937889×10^{-3}
16	2.916462×10^{-3}	2.026227×10^{-3}	3.597125×10^{-3}
17	2.456339×10^{-3}	1.809925×10^{-3}	3.298392×10^{-3}
18	2.075476×10^{-3}	1.614316×10^{-3}	3.035619×10^{-3}
19	1.758830×10^{-3}	1.438059×10^{-3}	2.803683×10^{-3}
20	1.494479×10^{-3}	1.279708×10^{-3}	2.598257×10^{-3}
21	1.272934×10^{-3}	1.137789×10^{-3}	2.415681×10^{-3}
22	1.086602×10^{-3}	1.010850×10^{-3}	2.252850×10^{-3}
23	9.293752×10^{-4}	8.974984×10^{-4}	2.107126×10^{-3}
24	7.963110×10^{-4}	7.964205×10^{-4}	1.976267×10^{-3}
25	6.833908×10^{-4}	7.063928×10^{-4}	1.858358×10^{-3}
26	5.873288×10^{-4}	6.262862×10^{-4}	1.751764×10^{-3}
27	5.054255×10^{-4}	5.550672×10^{-4}	1.655082×10^{-3}
28	4.354527×10^{-4}	4.917949×10^{-4}	1.567111×10^{-3}
29	3.755628×10^{-4}	4.356169×10^{-4}	1.486814×10^{-3}
Sum	2.265040×10^{-1}	7.204336×10^{-2}	1.511958×10^{-1}

CORRECTIONS FOR THERMAL BRIDGES

Some simple modifications were made to the building details in the vicinity of four of the bridges. Of the four bridge corrections considered only one could be feasibly applied as a retrofit, the others are only feasible to implement during construction. These modified bridges were analyzed with the finite-difference heat transfer code HEATING6. The resulting effective R-value, bridge conductance, and dimensionless interior temperature are presented in Table 5.

Rigid insulation is added to the sides of the concrete pillar constituting bridge 3. Two different insulation levels were used: 1 and 2 in. A similar type of correction could easily be applied to bridges 1 and 2.

The correction for bridge 4 consists of replacing the portion of the concrete floor slab directly underneath the stud wall with rigid insulation. The stud wall is not load bearing, and the rigid insulation need only be able to support the weight of the wall itself.

The steel studs of bridge 5 were replaced with fiberglass studs having a lower conductivity. However, the thickness of the fiberglass was greater than the steel, so the lower conductivity is partially offset by a larger heat flow area.

The correction for bridge 6 is similar to that for bridge 4. The grout making up the outer portion of the floor slab was replaced with rigid insulation. The steel deck underneath the grout was not removed since it is structurally required.

The type of information presented in Table 5 would enable building designers to make informed decisions concerning the inclusion of thermal bridges in a building.

Table 5. Results of thermal bridge corrective measures

Bridge No.	Modification	Effective R-value $\frac{h \cdot ft^2 \cdot °F}{Btu}$	Excess bridge conductance $\frac{Btu}{h \cdot °F}$	Excess bridge conductance $\frac{Btu/h \cdot °F}{ft\ of\ length}$	Minimum interior surface temperature Dimensionless
3	None	13.4	0.57	--	0.82
	1 in. insulation added	15.8	0.39	--	0.88
	2 in. insulation added	16.6	0.34	--	0.88
4	None	6.1	--	0.19	0.57
	Insulation replaces concrete	9.0	--	0.09	0.85
5	None	10.1	0.13	--	0.78
	Fiberglass replaces steel stud	11.0	0.10	--	0.83
6	None	6.5	--	0.26	0.74
	Insulation replaces grout	10.3	--	0.09	0.86

SUMMARY AND CONCLUSIONS

This report presents steady-state analyses of seven thermal bridges identified in a modern multistory commercial structure. Numerous finite-element and finite-difference heat transfer computer programs are readily available which are capable of performing comparable steady-state analyses. However, the use of any of these programs requires a fair degree of familiarity with the individual computer program and some knowledge of heat transfer in general and numerical heat transfer calculations in particular. No computer programs are generally available which are capable of performing meaningful dynamic analysis of thermal bridges. For these reasons it is desirable to develop a catalog of thermal bridges that gives the building designer adequate information to make informed decisions about the inclusion of thermal bridges in buildings. This report presents one possible approach for determining and presenting that information.

ACKNOWLEDGMENT

This work was done as part of the National Program for Building Envelope Systems and Materials for the Department of Energy, Office of Buildings Energy Research and Development.

REFERENCES

1. J. P. Silvers et al., *A Survey of Building Envelope Thermal Anomalies and Assessment of Thermal Break Materials for Anomaly Correction, Volume I - Survey and Assessment*, Dynatech R/C Company for Oak Ridge National Laboratory, ORNL/Sub/83-70376/1, July 1985.

2. B. S. Melton, et al., *Building Envelope Thermal Anomaly Analysis*, VVKR Inc. for Oak Ridge National Laboratory, ORNL/Sub/85-00294/1, December 1987.

3. D. C. Elrod, G. E. Giles, and W. D. Turner, *HEATING6: A Multidimensional Heat Conduction Analysis with the Finite-Difference Formulation*, ORNL/NUREG/CSD-2/V2, Oak Ridge National Laboratory, October 1981.

4. H. T. Ceylan and G. E. Myers, "Long-Time Solutions to Heat-Conduction Transients with Time-Dependent Inputs," *ASME J. of Heat Transfer*, **102** (February 1980).

5. S. E. Seem et al., "Transfer Functions for Efficient Calculation of Multidimensional Transient Heat Transfer, Heat Transfer in Buildings," *ASME HTD*, **78** (August 1987).

ORNL/TM-78
Dist. Category UC-95

INTERNAL DISTRIBUTION

1. J. G. Carbonell
2. R. S. Carlsmith
3-12. K. W. Childs
13. P. W. Childs
14. J. E. Christian
15. G. E. Courville
16. J. S. Crowell
17. W. Fulkerson
18. T. B. Kollie
19. M. A. Kuliasha
20. H. McLain
21. F. C. Maienschein
22. S. H. McConathy
23-37. S. D. Samples
38. S. H. McConathy
39. A. C. Schaffhauser
40. H. B. Shapira
41-43. C. H. Shappert
44. P. H. Shipp
45. J. N. Tunstall
46. G. E. Whitesides/R. P. Leinius/ Enrichment Technology Library
47. E. W. Whitfield
48. T. J. Wilbanks
49. K. E. Wilkes
50. Central Research Library
51. Document Records Section
52-54. Laboratory Records
55. Enrichment Technology Library
56. ORNL Patent Office
57. Plant Records (RC)

EXTERNAL DISTRIBUTION

58. P. R. Achenback, 1322 Kurtz Road, McLean, VA 22101
59. R. L. Alumbaugh, Naval Civil Engineering Laboratory, Port Hueneme, CA 93043
60. H. Amistadi, P. O. Box 904, Brunswick, ME 04011
61. T. Applegate, Applegate Insulation Systems, P.O. Box 292, Okemos, MI 48864
62. E. L. Bales, Building Engineering and Architectural Research Center, New Jersey Institute of Technology, Newark, NJ 07102
63. J. V. Beck, Michigan State University, Department of Mechanical Engineering, 205 Engineering Building, East Lansing, MI 48824
64. J. J. Boulin, Department of Energy, Buildings Division, CE-131 Forrestal, Washington, DC 20585
65. W. C. Brown, National Research Council of Canada, Ottawa, Ontario, Canada K1A OR6
66. M. Bomberg, National Research Council of Canada, Ottawa, Ontario, Canada K1A OR6
67. D. M. Burch, National Bureau of Standards, Building 226, Room B320, Gaithersburg, MD 20899
68. J. H. Cable, Cable-Menge Associates, 1580 Emerson Avenue, McLean, VA 22101

69. W. Carroll, Lawrence Berkeley Laboratory, Berkeley, Building 90, Room 2056, CA 94720
70. K. Cavanaugh, National Concrete Masonry Association, P. O. Box 781, Herndon, VA 22070
71. R. S. Dougall, University of Pittsburgh, Department of Mechanical Engineering, Pittsburgh, PA 15261
72. W. P. Ellis, Standards Consultant, 754 Bob-Bea Lane, Harleysville, PA 19436
73. D. M. Evans, Jr., Steven Winter Associates, Inc., 6100 Empire State Building, New York, NY 10001
74. D. R. Flynn, National Bureau of Standards, Sound Building, Room A147, Gaithersburg, MD 20899
75. W. R. French, Moisture Systems, Inc., 1233 West Loop South, Suite 1300, Houston, TX 77027-9108
76. F. C. Gorham, Roofing Services, Inc., 6106 Roxbury Avenue, Springfield, VA 22152-1621
77. W. P. Goss, University of Massachusetts, Mechanical Engineering Department, Amherst, MA 01003
78. J. Greko, Duro-Last Roofing, Inc., 525 Morley Drive, Saginaw, MI 48601
79. E. I. Griggs, Tennessee Technological University, Department of Mechanical Engineering, Cookeville, TN 38505
80. J. Harris, Bonneville Power Administration, Portland, Oregon.
81. R. O. Hinckley, University of Southwestern Louisianna, P.O. Box 44170, Lafayette, LA 70504
82. B. Howard, National Association of Homebuilders, 15th and M Street, N.W., Washington, DC. 20005
83. B. Hyma, Energy Saver Imports, Inc., 2150 West 6th Avenue - Unit E, P.O. Box 387, Broomfield, CO 80020
84. C. W. Jennings, Tennessee Valley Authority, 3557D-C Signal Place, 1101 Market Street, Chattanooga, TN 37402-2801
85. F. R. Kalhammer, Energy Management and Utilization Division, Electric Power Research Institute, 3412 Hillview Avenue, P. O. Box 10412, Palo Alto, CA 94303
86. R. E. Kasperson, Graduate School of Geography, Clark University, Worcester, MA 01610
87. J. Klems, Lawrence Berkeley Laboratory, Building 90, Room 3111, Berkeley, CA 94720
88. W. M. Kroner, Rensselaer Polytechnic Institute, Center for Architectural Research, Troy, NY 12181
89. R. J. Kudder, Raths, Raths and Johnson, Inc., 835 Midway Drive, Willowbrook, IL 60521
90. M. B. Lacher, Certainteed Corporation, P.O. Box 860, Valley Forge, PA 19482
91. R. A. Lacosse, National Roofing Contractors Association, One O'Hare Centre, 6250 River Road, Rosemont, IL 60018
92. E. Leger, P. O. Box 549, New Boston, NH 03070
93. M. D. Lyberg, Swedish Institute of Buildings, Box 785, S-801 29, Gavle, Sweden.
94. P. C. Martin, Manville Service Corporation, Denver, Research and Development Center, P.O. Box 5108, Denver, CO 80217
95. M. McBride, Owens-Corning Fiberglas, Technical Center, P.O. Box 415, Granville, OH 43023

96. D. McGuire, Regal Industries, Route 1, Box 46, Crothersville, IN 47229
97. K. Mentzer, Mineral Insulation Manufacturing Assoc., 1420 King Street, Alexandria, VA 22314
98. G. Miller, Jim Walter Research Corporation, 10301 9th Street, North, St. Petersburg, FL 33716
99. P. G. Mulroney, 4557 King Edward Court, Annandale, VA 22003
100. N. Nisson, Energy Design Update, P.O. Box 1709, Ansonia Station, New York, NY 10023
101. E. Nowman, Fi-Foil Company, Inc., P.O. Box 7046, Winter Haven, FL 33883
102. R. L. Perrine, Engineering and Applied Sciences, Civil Engineering Department, Room 2066, University of California Los Angeles, Los Angeles, CA 90024
103. D. E. Richards, Owens-Corning Fiberglas Corp., Toledo, OH 43659
104. W. J. Rossiter, National Bureau of Standards, Gaithersburg, MD 20899
105. J. A. Roux, University of Mississippi, Department of Mechanical Engineering, University, MS 38677
106. J. Samos, NASA-Langley Research Center, Mail Stop 139A, Hampton, VA 23665-5225
107. E. Schaffer, U.S. Forest Products Laboratory, One Gifford Pinchot Drive, Madison, WI 53704-2398
108. R. C. Schroter, Product Technical Service Associates, 120 Village Square, Suite 121, Orinda, CA 94563
109. S. Selkowitz, Lawrence Berkeley Laboratory, Building 90, Room 3111, Berkeley, CA 94720
110. M. Sherman, Jim Walter Corporation, 10301 9th Street North, St. Petersburg, FL 33702
111. C. J. Shirtliffe, Building Services, National Research Council of Canada, Building M-24, Ottawa, Ontario, Canada K1A OR6
112. J. A. Smith, Department of Energy, CE-131 Forrestal, Washington, DC 20585
113. L. G. Spielvogel, Wyncote House, Wyncote, PA 19095-1499
114. R. Sterling, University of Minnesota, Underground Space Center, 790 Civil and Mineral Engineering Building, 500 Pillsbury Drive, S.E., Minneapolis, MN 55455
115. G. A. Tsongas, Portland State University, Department of Mechanical Engineering, P.O. Box 751, Portland, OR 97207
116. A. Tuluca, Steven Winter Associates, 50 Washington Street, 6th Floor, Norwalk, CT 06854
117. R. P. Tye, Dynatech Scientific, Inc., 99 Erie Street, Cambridge, MA 02139
118. M. G. Van Geem, Construction Technology Laboratories, Inc., Portland Cement Assoc., 5420 Old Orchard Road, Skokie, IL 60077
119. C. R. Vander Linden, Vander Linden and Associates, 5 Brassie Way, Littleton, CO 80123
120. B. Wilcox, Berkeley Solar Group, Berkeley, CA
121. Office, Assistant Manager, Energy Research and Development, 200 Administration Road, Federal Building, Oak Ridge, TN 37830

122-131. Office of Scientific and Technical Information, P.O. Box 62, Oak Ridge, TN 37830